Supplementary Information Titles

Please upload this form (in Word format) as a "Related Manuscript File".

Note that we do NOT copy edit or otherwise change supplementary information, and minor (nonfactual) errors in these documents cannot be corrected after publication. Please submit document(s) exactly as you want them to appear, with all text, images, legends and references in the desired order, and check carefully for errors.

Journal: Nature Neuroscience

Article Title:	Betaine acts on a ligand-gated ion channel in the nervous system of the nematode *C. elegans*
Corresponding Author:	Erik M Jorgensen

Please list each supplementary item and its title or caption, in the order shown below.

Supplementary Item & Number (add rows as necessary)	**Title or Caption**
Supplementary Figure 1	*snf-3* gene and expression pattern
Supplementary Figure 2	The suppressor *ox429* is an allele of *acr-23*
Supplementary Figure 3	SNF-3 transports betaine in *Xenopus* oocytes.
Supplementary Figure 4	A model for betaine function in *C. elegans*.

Betaine acts on a ligand-gated ion channel in the nervous system of the nematode *C. elegans*

Aude S. Peden[1], Patrick Mac[1*], You-Jun Fei[2*], Cecilia Castro[3,4], Guoliang Jiang[2], Kenneth J. Murfitt[3,5] , Eric A. Miska[3,5], Julian L. Griffin[3,4,6], Vadivel Ganapathy[2], Erik M. Jorgensen[1,7]

1. Howard Hughes Medical Institute, Department of Biology, University of Utah, Salt Lake City, UT 84112, USA
2. Departments of Biochemistry and Molecular Biology, Georgia Regents University, Augusta, GA USA 30912, USA
3. Department of Biochemistry, University of Cambridge, Tennis Court Rd, Cambridge CB2 1GA, UK
4. Cambridge Systems Biology Centre, University of Cambridge, 80 Tennis Court Road, Cambridge, CB2 1GA, UK
5. Wellcome Trust Cancer Research UK Gurdon Institute, University of Cambridge, The Henry Wellcome Building of Cancer and Developmental Biology, Tennis Court Rd, Cambridge CB2 1QN, UK
6. The Medical Research Council Human Nutrition Research, Elsie Widdowson Laboratory, Fulborn Road, Cambridge, CB1 9NL, UK
7. Corresponding author: Erik M. Jorgensen, (801) 585-3517 (phone), (801) 585-3517 (fax), jorgensen@biology.utah.edu

* contributed equally to this work

Supplementary materials: 4 Figures

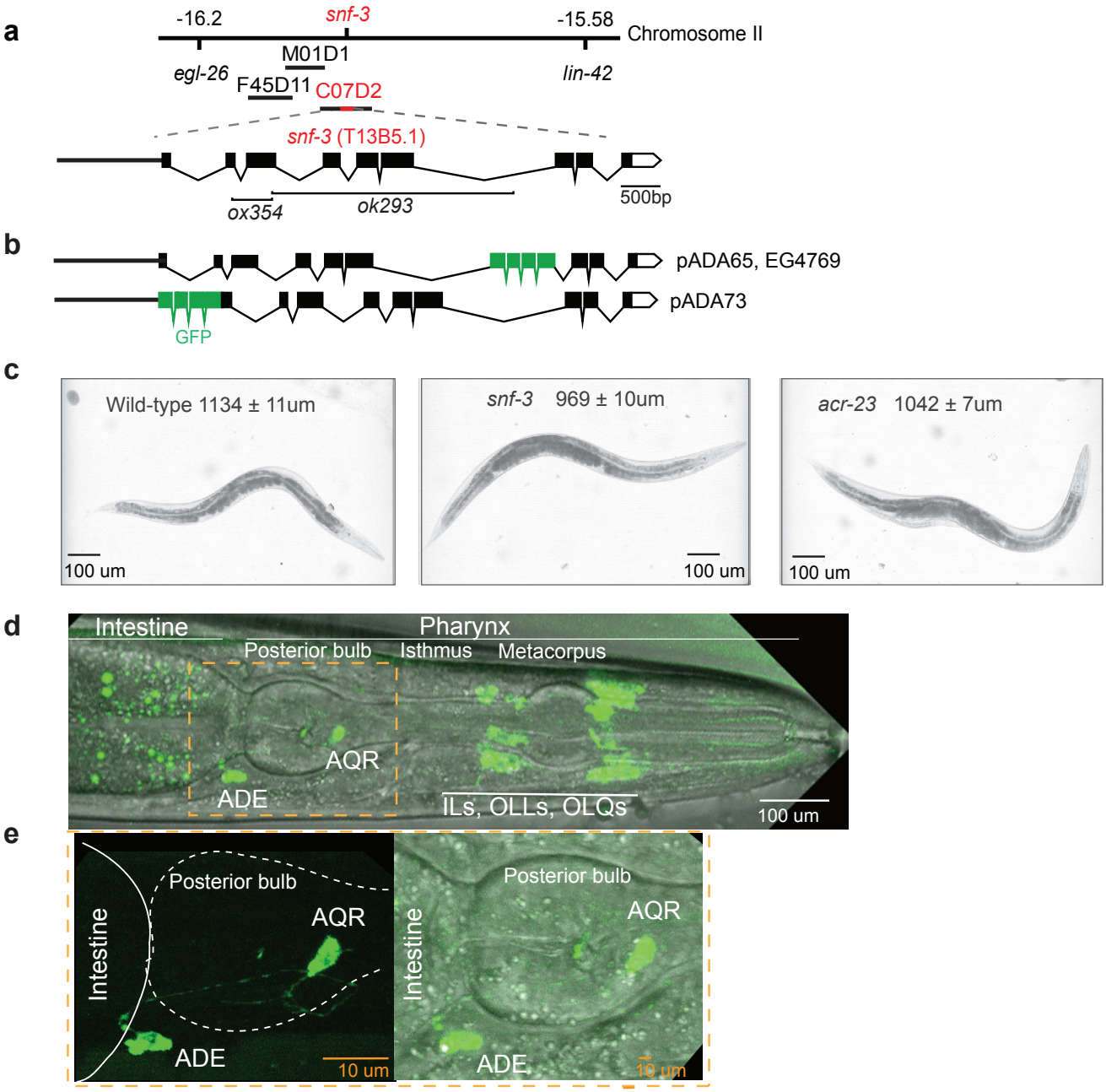

Supplementary Figure 1: *snf-3* gene and expression pattern.
(**a**) Genetic map and structure of the *snf-3* gene. The gene was identified by mapping *snf-3(ox354)* using single nucleotide polymorphisms and transgenic rescue. The *snf-3* locus maps to the left arm of chromosome II in a region covered by three cosmids, F45D11, M01D1 and C07D2. C07D2 and the gene T13B1.5 rescued the hypercontracted phenotype. T13B1.5 encodes the *snf-3* gene. *ox354* and *ok293* are deletion alleles. In *snf-3(ox354)* exons 2-3 are deleted, in *snf-3(ok293)* exons 3-6 are deleted. (**b**) pADA65 and pADA73 are the two SNF-3-GFP fusion plasmids used to determine SNF-3 expression and subcellular localization. EG4769 is a transgenic rescue strain injected with pADA65. (**c**) Representative images of adult hermaphrodites. *snf-3* and *acr-23* mutants alone are morphologically wild-type. *acr-23(-)* suppresses the *snf-3(-)* contribution to the *snf-3 egl-8* double mutant; that is, *acr-23 snf-3 egl-8* triple mutant resembles the *egl-8* single mutant. Values represent the mean length of a young adult animal for each genotype ± s.e.m. (**d**) SNF-3 is expressed in a limited set of neurons. The transgenic strain EG4769 carrying P*snf-3::SNF-3::GFP::snf-3*utr (also used in Figure 3a) was grown on RNAi against GFP to reveal neuronal expression. Neurons are resistant to the effects of RNAi. *snf-3*-expressing neurons in the head are the non-amphidial sensory neurons: 19 cell bodies around the metacarpus of the pharynx were identified as inner (ILs) and outer (OL) labial neurons based on cell body and dendrite positions. OLL= outer labial lateral, OLQ = outer labial quadrant. ADE was identified based on its position behind the posterior bulb of the pharynx, and AQR because this neuron is unilateral. * indicates unidentified neuron. (**e**) An enlargement of the posterior bulb region showing the morphology of the ADE and AQR neurons.

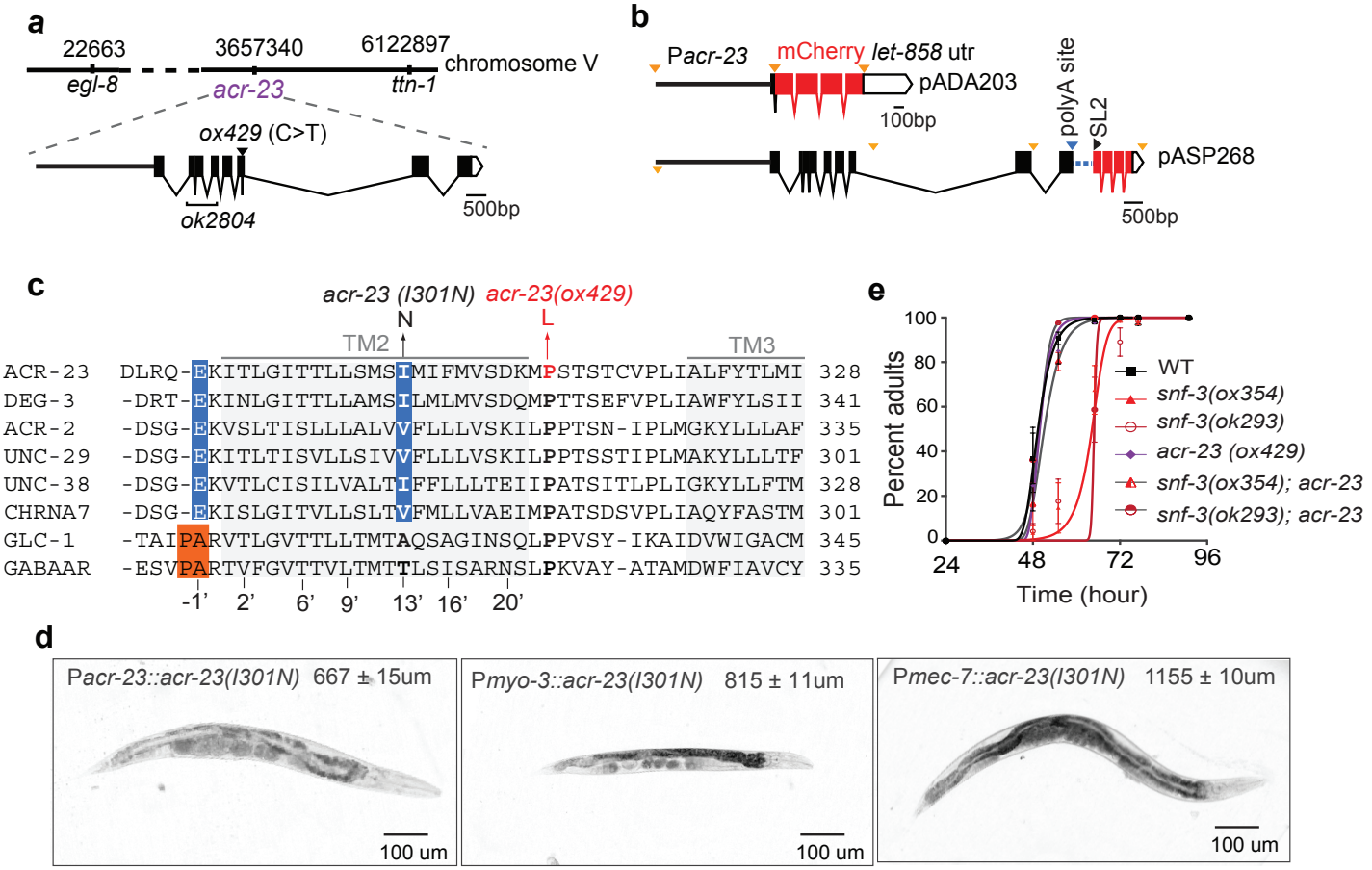

Supplementary Figure 2: The suppressor *ox429* is an allele of *acr-23.*
(a) *ox429* is an allele of *acr-23*, which encodes a cys-loop ligand-gated ion channel gene. The mutation *ox429* was identified using genome-wide Illumina sequencing of *snf-3 egl-8 ox429* triple mutant (EG6501). 448 single nucleotide polymorphisms (SNPs) were identified compared to the reference Bristol N2 genomic sequence. We found that 407 of these substitutions were either in non-coding sequences or were synonymous substitutions (silent changes at the amino acid level). We focused on the 41 SNPs with non-synonymous substitutions for further analysis. One SNP was contained in the *acr-23* gene, a nematode-specific cys-loop ligand-gated ion channel. The *ox429* is a C to T transition that causes the missense change P311L in the open reading frame. We confirmed that this change is the suppressor mutation by transgenic rescue and by crossing the null allele *acr-23(ok2804)* into the *snf-3 egl-8* double mutant. **(b)** pADA203 and pASP268 are transcriptional mCherry fusion plasmids used to determine the *acr-23* expression pattern. The yellow triangles denote Gateway (attB) recombination sites. For pASP268, we used the intergenic region of the *gpd-2 gpd-3* operon (dotted blue line) to express mCherry in an operon with the entire *acr-23* gene. The blue and black triangles denote the polyA site and the SL2 transplice acceptor site. **(c)** Alignment of the mutated region of ACR-23 with selected cys-loop ligand-gated ion channels. *C. elegans* AcetylCholine Receptor family member-23 (ACR-23; NP_504024.2); *C. elegans* Degeneration of certain neurons-3 (DEG-3; NP_505897.1); *C. elegans* AcetylCholine Receptor family member-2 (ACR-2; NP_509128.1); *C. elegans* UNCoordinated family member-29 (UNC-29; NP_492399.1); *C. elegans* UNCoordinated family member-38 (UNC-38; NP_491472.1); Human neuronal acetylcholine receptor subunit alpha-7 (CHRNA7; NP_001177384.1); *C. elegans* Glutamate-gated Chloride channel 1 (GLC-1; NP_507090.1); Human GABA-A alpha-1 (GABA-AR CAA32874.1). The residues that distinguish cation (blue) and anion (orange) selectivity for ligand-gated ion channels are highlighted. The C to T mutation in *ox429* converts a proline at position 311 to a leucine. This proline is conserved in all cys-loop ligand-gated channels and is required for receptor function (Deane CM *et. al.*, JBC, 2001). Mutations of the 13' position of the second transmembrane domain of two *C. elegans* receptors, *deg-3(u662)* (Treinin M *et. al.,* Neuron, 1995) and *acr-2(n2420)* (Jospin M *et. al.,* PloS Biol, 2009), cause a gain-of-function phenotype. We engineered an ACR-23 gain-of-function mutation based on the *deg-3(u662)* mutation in which an isoleucine was replaced by an asparagine (I301N). **(d)** Transgenic worms expressing an *acr-23(I301N)* gain-of-function receptor. P*myo-3* drives expression in body wall muscles. P*mec-7* drives expression in mechanosensory neurons. Behavioral analyses of these worms are shown in Figure 5 e-f. **(e)** *acr-23* suppresses *snf-3* growth defects. We measured the time from embryo to young adult. Egg-laying was synchronized by transferring parents to new plates every 6 hours. (mean of five independent assays ± s.e.m; *n*= 500 worms per experiment for each genotype). The data were fitted using KaleidaGraph 3.6 software.

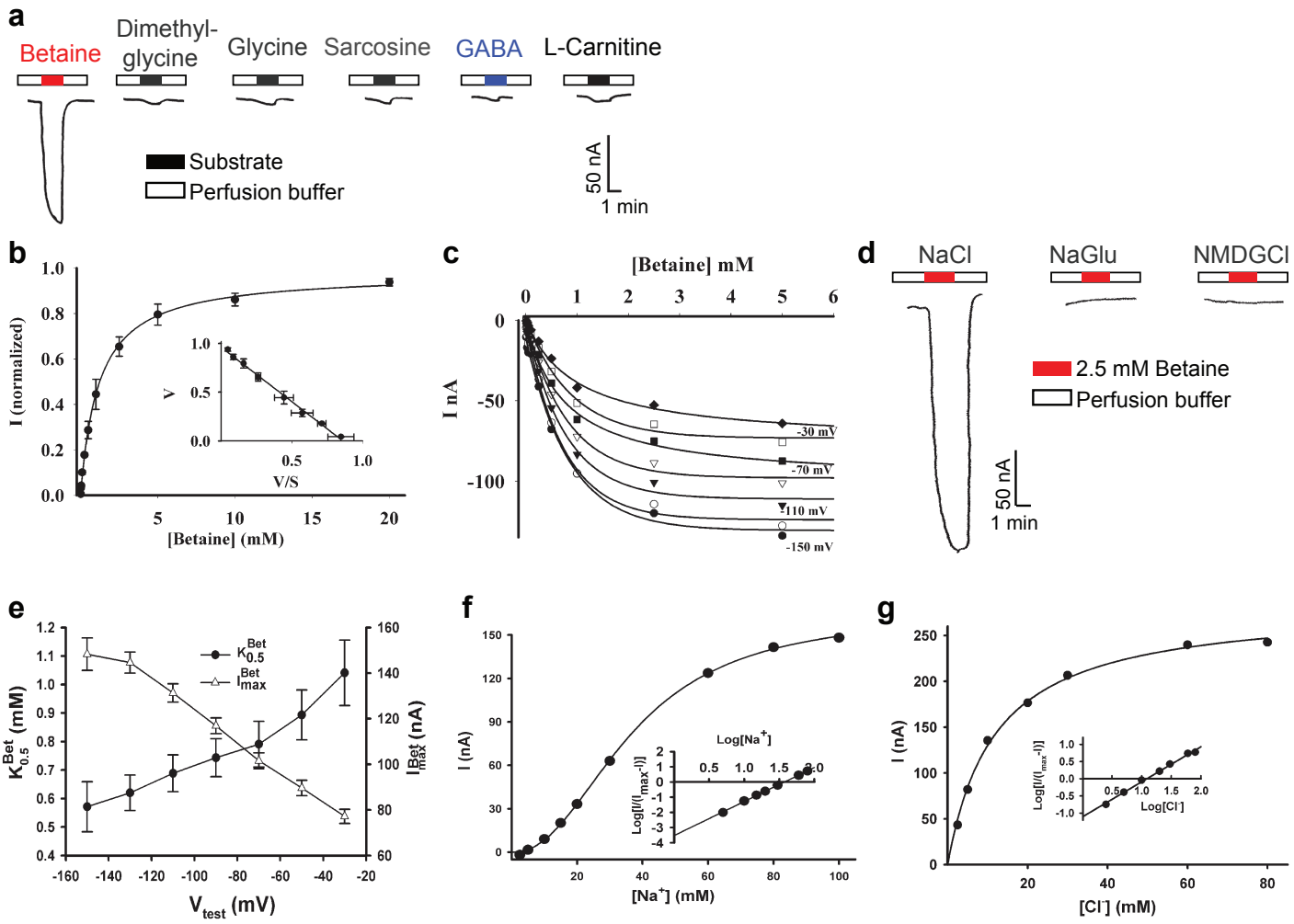

Supplementary Figure 3: SNF-3 transports betaine in *Xenopus* oocytes.
(**a**) Substrate specificity of SNF-3 in *Xenopus* oocytes. Representative current traces induced by 2.5 mM betaine, dimethylglycine (DM-glycine), glycine, sarcosine (methylglycine), GABA or L-carnitine in oocytes expressing SNF-3. **(b)** Saturation kinetics of SNF-3 activity. Betaine uptake conformed to Michaelis-Menten kinetics at each tested membrane potential (Inset: Eadie-Hofstee conversion of the same saturation data (v/s): [betaine uptake velocity (v) versus betaine uptake velocity/betaine concentration (v/s)). Betaine-induced currents were tested at a membrane potential of –50 mV and were normalized and fitted by non-linear regression (n=3 oocytes). Results are presented as mean ± SEM. **(c)** Betaine-induced currents are saturable over a range of membrane potentials. Representative recordings from each membrane potential tested. We used voltage steps to measure currents ranging from -30mV to -150mV. **(d)** SNF-3-mediated current is dependent on Na^+ and Cl^- ions. Chloride ions were replaced by gluconate (NaGlu), and sodium ions were replaced by N-methyl-D-glucamine (NMDGCl). **(e)** SNF-3 activity is regulated by membrane potential. Voltage-dependence of SNF-3 was determined by gradually changing membrane potential from –30 mV to –150 mV. The substrate-induced maximal current (I^{Bet}_{max}) increased from 77 ± 3 nA to 148 ± 7 nA and the Michaelis constant ($K^{Bet}_{0.5}$) changed from 1.0 ± 0.1 mM to 0.6 ± 0.1 mM. Kinetic parameters, $K_{0.5}$ and I_{max}, were determined at varying membrane potentials from three different oocytes after normalization. Results are presented as mean ± SEM. **(f,g)** Activation kinetics for SNF-3-mediated betaine transport by Na^+ **(f)** and Cl^- **(g)** Inset: Hill plot of SNF-3 affinities for Na^+ and Cl^- and their respective Hill coefficients (*h*) were determined at – 50 mV using the Hill equation. n= 3 oocytes for each ion. The Michaelis constant of SNF-3 for sodium ($K^{Na}_{0.5}$) was 37 ± 1 mM with a Hill coefficient of 2.2 ± 0.1, and the corresponding value for chloride ($K^{Cl}_{0.5}$) was 12 ± 1 mM with a Hill coefficient of 1.0 ± 0.1.

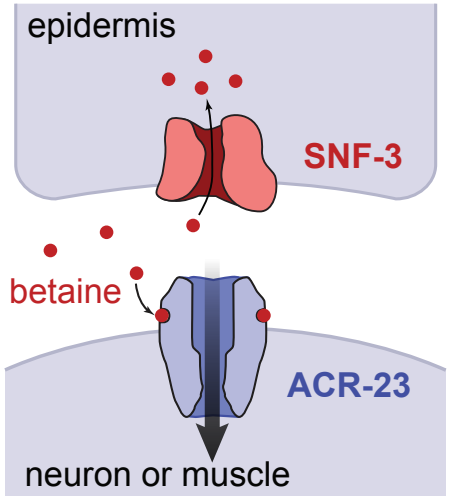

Supplementary Figure 4. A model for betaine function in *C. elegans.*
The SNF-3 transporter functions in the epidermis to limit betaine in the extracellular space.
The betaine receptor ACR-23 acts in a subset of neurons to regulate basal levels of locomotion.